HHS Public Access

Author manuscript

J Immunol. Author manuscript; available in PMC 2019 November 01.

Published in final edited form as:

J Immunol. 2018 November 01; 201(9): 2710–2720. doi:10.4049/jimmunol.1800365.

Perforin-2 Breaches the Envelope of Phagocytosed Bacteria Allowing Antimicrobial Effectors Access to Intracellular Targets

Fangfang Bai, **Ryan M. McCormack**, **Suzanne Hower**, **Gregory V. Plano**, **Mathias G. Lichtenheld**, and **George P. Munson***

Department of Microbiology and Immunology, Miller School of Medicine, University of Miami, Miami, 33163 USA

Abstract

Perforin-2, the product of the *MPEG1* gene, limits the spread and dissemination of bacterial pathogens in vivo. It is highly expressed in murine and human phagocytes, and macrophages lacking Perforin-2 are compromised in their ability to kill phagocytosed bacteria. In this study we used *Salmonella enterica* serovar Typhimurium as a model intracellular pathogen to elucidate the mechanism of Perforin-2's bactericidal activity. In vitro Perforin-2 was found to facilitate the degradation of antigens contained within the envelope of phagocytosed bacteria. In contrast, degradation of a representative surface antigen was found to be independent of Perforin-2. Consistent with our in vitro results a protease sensitive, periplasmic superoxide dismutase (SodCII) contributed to the virulence of *S.* Typhimurium in Perforin-2 knockout but not wild-type mice. In aggregate our studies indicate that Perforin-2 breaches the envelope of phagocytosed bacteria facilitating the delivery of proteases and other antimicrobial effectors to sites within the bacterial cell.

Introduction

Macrophages and neutrophils phagocytose microorganisms to remove them from blood and tissues. As the phagosome matures the multisubunit NADPH oxidase assembles on its membrane and reduces O_2 to generate superoxide in the lumen of the phagosome (1, 2). The products of this respiratory burst –superoxide and subsequently other reactive oxygen species (ROS)– are bactericidal. The destruction and degradation of phagocytosed microbes is further facilitated by acidification of the phagosome and fusion with lysosomes that deliver oxygen-independent antimicrobial effectors such as lysozyme, glycosylases, proteases, and other hydrolases (3). Large antimicrobials such as proteases and other hydrolases are typically membrane impermeable molecules. This property is advantageous in that it allows them to be confined within lysosomes and phagolysosomes. However it also

*Correspondence: George P. Munson, Tel: 305-243-5317, gmunson@miami.edu.

Conceptualization, F.B., R.M.M., M.G.L., and G.P.M.; Methodology, F.B., R.M.M., and G.P.M.; Investigation, F.B.; Validation, F.B and G.P.M.; Formal Analysis, F.B.; Resources, S.H., G.V.P., and R.M.M.; Writing – Original Draft, F.B. and G.P.M.; Writing – Review & Editing, F.B., R.M.M., S.H., G.V.P., M.G.L., and G.P.M.; Visualization, F.B. and G.P.M.; Supervision, M.G.L. and G.P.M.; Funding Acquisition, G.P.M.

Declaration of Interests

The authors declare no competing interests.

precludes them from reaching the internal components of phagocytosed bacteria. For example, lysozyme hydrolyzes β(1,4)-glycosidic bonds of peptidoglycan; the primary structural component of bacterial cell walls. In gram-negative bacteria peptidoglycan resides in the space between the outer and inner membranes; i.e., the periplasm. Thus, for these bacteria a breach of the outer membrane must precede lysozyme-dependent degradation of peptidoglycan (4, 5). For hydrolases with targets in the cytosol of gram-negative bacteria the challenge is two-fold as their substrates are bound by both an inner and outer membrane.

Studies over the past two decades have shown that antimicrobial peptides such as the defensins and cathelicidins attack and disrupt bacterial membranes (6–9). Nuclear magnetic resonance studies of the cathelicidin LL-37 suggest that the peptide destabilizes the bacterial membrane by carpeting rather than penetrating the lipid bilayer (10). Within phagolysosomes the murine cathelicidin (CRAMP) has been shown to be active against phagocytosed *Salmonella*; most likely by disruption of the bacterium's outer membrane (11, 12). Likewise, cathelicidin LL-37 may play a similar role in human phagocytes (13, 14). Nearly coincident with the initial descriptions of LL-37 and CRAMP the *Mpeg1* gene was identified as a potential marker of mammalian macrophages due to its relatively high expression in mature human and murine macrophages (6, 15, 16). *Mpeg1* encodes a 73 kDa protein referred to as Perforin-2 and in their initial report Spilsbury et al. noted its partial homology to the MACPF domain of Perforin; the cytolytic protein of natural killer cells and cytotoxic T lymphocytes (15). Unlike the carpet mechanism of cathelicidins Perforin is a large polypeptide that polymerizes on target membranes. A concerted structural transition results in a pore through the lipid bilayer whose hydrophilic channel is lined with amphipathic β-strands donated by the MACPF domains (17, 18). It is through this channel, either at the cell surface as originally hypothesized or within endosomal membranes as a more recent study suggest, that granzyme proteases enter tumor and virally infected cells to facilitate their destruction and lysis (19–21). MACPF domains are also present in the terminal complement proteins which form pores in the outer membranes of gram-negative bacteria through a similar mechanism of polymerization and structural transition (22).

Despite the homology of mammalian Perforin-2 to known pore forming proteins there was no further elaboration of its function until 2013; nearly two decades after the initial report of Spilsbury et al.(15, 23). In 2013 McCormack et al. demonstrated that the expression of Perforin-2 correlated with the killing of phagocytosed gram-negative, -positive, and acid-fast bacteria in vitro (23). Subsequent studies with transgenic mice found that Perforin-2 knockout (KO) mice are unable to limit the proliferation and dissemination of infectious bacteria. Not surprisingly, Perforin-2 KO mice succumb to infectious doses that are non-lethal to their wild-type (WT) littermates (24–26). Moreover this defect is not limited to a particular route of infection nor pathogen. Nor is it limited to mammalian Perforin-2 as similar results have been reported with zebrafish as the model organism (27). In aggregate these latter studies have demonstrated that Perforin-2 is associated with broad spectrum bactericidal activity. In this study we utilized *Salmonella enterica serovar* Typhimurium (*S.* Typhimurium) as a model pathogen to elucidate the mechanism of Perforin-2 dependent killing of phagocytosed bacteria.

Material and Methods

Mice

Perforin-2 KO 129X1/SvJ mice were produced at the University of Miami Miller School of Medicine Transgenic Core Facility as previously described (24). WT 129X1/SvJ and Perforin-2 KO mice of either sex were used at 2 to 6 months of age. Mice received food and water *ad libitum* and were housed at an ambient temperature of 23°C on a 12 h light/dark cycle under specific pathogen-free conditions. Mice were euthanized by CO_2 inhalation followed by cervical dislocation. All procedures with animals were reviewed and approved by the University of Miami's Institutional Animal Care and Use Committee.

Strains and Plasmids

Bacterial strains are listed in Table 1. Primer sequences are listed in Table 2. Strains constructed for this study are isogenic derivatives of *S.* Typhimurium strain LT2 (28). Plasmid pKD4 (29) was used in PCR with primer pairs sodCI-P1/sodCI-P2 or sodCII-P1/sodCII-P2 to generate kanamycin resistance cassettes bracketed by recognition sites for FLP recombinase and flanking sequences targeting *sodCI* or *sodCII*. Deletions of *sodCI* or *sodCII* were generated by λRed-mediated recombination of the cassettes into LT2 as described (29). Recombinants were selected on Luria-Bertani (LB) agar plates with kanamycin. Recombination sites were verified by PCR with flanking primer pairs sodCI-MfeI/sodCI-HindIII for *sodCI::kan* and sodCII-EcoRI/sodCII-HindIII for *sodCII::kan*. For the construction of double deletions FLP recombinase was used to excise the first cassette prior to insertion of the second.

The *sodCII* gene was cloned from LT2 by PCR with primers 1238/1239. The PCR product was digested with XbaI and BamHI then ligated into the same sites of pAH63Tc, a derivative of pAH63 (30) in which the kanamycin resistance gene was replaced with one conferring resistance to tetracycline. To complement *sodCII* mutants the resulting plasmid, pAH63Tc-sodCII, was integrated into $attB_\lambda$ of relevant strains by a site specific recombinase as previously described (30). The chloramphenicol resistant strain GPM2004 was constructed by integration of pCAH63 (30) into $attB_\lambda$ of LT2. Plasmid pTrc99aSodCII3flag was constructed by HiFi DNA assembly (New England Biolabs) of three PCR products: one carrying *sodCII* amplified from pAH63Tc-sodCII with primers 1329/1330, another carrying a triple FLAG epitope amplified from pSUB11 (31) with primers 1331/1332, and the vector backbone amplified from pTrc99a (32) with primers 1333/1334. Bacteria were cultured in LB broth or plates. Genes encoding Perforin-2 and E2-Crimson were cloned into the dual expression plasmid pVitro1-neo-Lucia-SEAP (InvivoGen) by HiFi assemble with the primer pairs 1426/1427, 1584/1585 and 1586/1587. The new construction was named pMuP2-E2-Crimson. The superfold green fluorescent protein expressing strains were constructed by integration of pCAH63-sfGFP, which was assembled by HiFi with primer pairs 1258/1259 and 1257/1243, into $attB_\lambda$ of relevant strains. The pBAD-TurboRFP plasmid (Addgene) was electroporated into LT2 for constructing the S. Typhimurium LT2 / pBAD-TurboRFP. As appropriate antibiotics were used at the following concentrations: chloramphenicol, 10 μg/ml; ampicillin, 100 μg/ml; kanamycin, 50 μg/ml; tetracycline 7.5 μg/ml.

Cell preparation

Peritoneal exudate macrophages (PEMs) were isolated as previously described (33). Briefly, mice were injected intraperitoneally with 1 ml of 4% Brewer thioglycollate medium and peritoneal exudates were recovered after 4 days. A modified schedule was used to collect PEMs for ROS assays (34). In brief, mice were inoculated on days 1 and 7, and exudates were collected on day 14. Resting macrophages were collected from the peritoneal cavities of untreated mice. Peritoneal neutrophils were elicited and recovered as previously described (35). Briefly mice were injected intraperitoneally with 1 ml 9 % casein in PBS (2.7 mM KCl, 4.3 mM Na_2HPO_4, 1.47 mM KH_2PO_4, 137 mM NaCl, pH 7.4) containing 0.9 mM $CaCl_2$ and 0.5 mM $MgCl_2$. A second injection was administered 16 h after the first and exudates collected 3 h later. Cells were maintained in IMDM (Gibco) supplemented with 10 % FBS (Gibco) at 37°C in 5% CO2. Bone marrow derived macrophage (BMDM) were isolated from the femurs from the Perforin-2 WT and KO mice. The cells were cultured in IMDM medium supplemented with 10% FBS, 20% L929 conditioned medium, and 10 mM L-glutamine. BMDM were cultured for 6 days before use, and the culture medium was changed every 2 days.

Intracellular killing assays

Intracellular gentamicin protection assays were performed as previously described (23, 36, 37). Briefly, 3×10^5 PEM were seeded in 24 well plates in IMDM, 10 % FBS and incubated at 37°C in 5% CO_2. Murine IFN-γ (Biolegend) was added 14 hours before infection at a final concentration of 50 ng/ml. Overnight cultures of bacteria were diluted 33 fold in LB and cultured aerobically at 37°C for 3 hours to mid-log at which point the optical absorbance of the culture at 600 nm was ca. 0.6. Bacteria were added at a multiplicity of infection between 20 to 50 and plates incubated for 45 to 60 min to allow for uptake of bacteria. Cells were then washed three times with PBS and fresh culture medium containing 50 μg/ml gentamicin was added to each well to kill extracellular bacteria. After 2 hours the concentration of gentamicin was reduced to 5 μg/ml. At selected time points gentamicin was removed by PBS washes and bacteria were recovered by lysis of mammalian cells in sterile water with 0.1% Triton X-100. Lysates were serially diluted in PBS and the bacteria were enumerated on LB agar plates.

ROS detection

3×10^5 PEM were seeded in 96-well opaque white plates in 200 μl of phenol red–free IMDM, 10% FBS and primed for 14 hours with murine IFN-γ at a final concentration of 50 ng/ml. Alternatively, 3×10^5 neutrophils were seeded in KRPG buffer (145 mM NaCl, 4.86 mM KCl, 5.7 mM sodium phosphate, 0.54 mM $CaCl_2$, 1.22 mM $MgSO_4$, 5.5 mM Glucose, pH 7.35). For ROS production in neutrophils, cells were incubated with 1 mM luminol (Sigma) for 3 min. before adding PMA (InvivoGen) or LPS (InvivoGen) to a final concentration of 100 ng/ml. Some wells were treated with 10 nM diphenyleneiodonium chloride (DPI) (Sigma) –a NAPDH oxidase inhibitor– for 30 min prior to addition of luminol. The same procedures were used with macrophages except the luminol enhancer Diogenes (National Diagnostics) was also used (38). For the measurement of phagocytic ROS production, 3 μm amino microspheres polybeads (Polysciences Inc.) were treated with

8% glutaraldehyde in PBS overnight at room temperature with agitation. Beads were washed with PBS, incubated with 100 mM luminol in DMSO for 4 hours at room temperature and subsequently washed with 0.5 M glycine and PBS. Prepared the beads were stored in PBS. Perforin-2 WT or KO neutrophils were pulsed with luminol-coupled beads for 15 min and then washed with PBS. When indicated, 0.5 μg/ml PMA was added before starting. Luminescence was recorded in an EnVision (PerkinElmer) plate reader.

Measurement of vacuolar pH

The pH of *Salmonella* containing vacuoles (SCVs) was determined as previously described (39) with modifications. Perforin-2 WT or KO PEMs were seeded on 8 well slides (IbITreat μ-Slide, Ibidi USA Inc.) at 50,000 cells per well and incubated overnight. The cells were then loaded with dextran-FITC MW 10,000 at 282 μg/ml and dextran-Alexa Fluor 647 MW 10,000 at 70 μg/ml in normal growth medium for 4 h, then infected with TurboRFP expressing *S.* Typhimurium WT LT2 / pBAD-TruboRFP. After 1 hour cells were washed with HBSS containing 0.5% FBS and imaged in CO_2 independent medium with 10% FBS by fluorescent microscopy. The ratio of the two fluorophores (488/647 nm) within SCVs was quantified with the Fiji build of ImageJ (40). To generate a standard curve, the same cells used for experimental measurement were incubated with ionophore nigericin (20 μM, sigma) for 5 min at room temperature to allow the free exchange of H^+ ions across membranes and then with a series of buffers of varying pH (4.0–7.0). The pH standard buffers contained 140 mM KCl and 5 mM glucose buffered with 15 mM Tris for pH 7.0, 15 mM MES for pH 6.0, and acetic acid for pH 4.0 and 5.0.

Recovery of phagocytosed bacteria and immunodetection

S. Typhimurium LT2 /pTrc99aSodCII3flag was cultured aerobically overnight in LB with ampicillin at 37°C. The bacteria were pelleted, washed with sterile PBS and aliquots of the inoculum were frozen at −80 °C for later analysis. Aliquots of the inoculum were also used to infect WT and Perforin-2 KO PEMs at a multiplicity of infection of about 20–50. After 1 hour incubation, the cells were washed three times with PBS then IMDM with 10% FBS and 50 μg/ml gentamicin was added to each well. This initial addition of gentamicin marked the 0 hour time point. After 2 hours the concentration of gentamicin was decreased to 5 μg/ml. After 18 hours the cells were washed with PBS three times, then PBS, 0.1% Triton-X 100 containing a proteinase inhibitor cocktail (Roche) was added to each well. After a 5 min. incubation at 37°C the cells were manually detached with a cell scraper, the bacterial cells were harvested by centrifuged at 4°C at 10, 000 *g* × 10 min, and the supernatant was removed. Recovered phagocytosed bacteria (approximate 10^6 CFU) and bacteria from the original LB culture were boiled in Laemmli loading buffer for 7 min. The same infection procedure was conducted with WT and Perforin-2 KO BMDMs except the phagocytosed bacteria were collected at 1, 3 and 6 hours. The protein samples were separated on 4–20% gradient SDS-PAGE gels and transferred to nitrocellulose membranes. The membranes were blocked with 5% non-fat milk in Tris buffered saline containing 0.1% Tween-20 (TBST) for 2 hours and then incubated at 4°C for 16 hours with primary antibodies anti-FliC (1:1000, InvivoGen, Cat: 629701), anti-FLAG (1:5000, Sigma, Cat: F1804) or anti-DnaK (1:5000, Abcam, Cat: ab69617) diluted in TBST with 5% non-fat milk. After three washes with TBST the membranes were incubated at 37°C for 1 hour with anti-mouse horseradish

peroxidase-labeled secondary antibody (Jackson ImmunoResearch Laboratories, Cat: 115–036-062) diluted 1:5000 in TBST with 5% non-fat milk. An Odyssey FC Imaging System (LI-COR) was used to detect and quantify chemiluminescence after addition of SuperSignal West Pico Chemiluminescent Substrate (Thermo Fisher Scientific).

Cofocal microscopy

RAW264.7 cells were transfected with pMuP2-E2-Crimsion plasmid with Lipofectamine LTX (Invitrogen) following the manufacturer's instructions. The transfected cells were seeded on 25-mm coverslips, the cells were infected with superfold green fluorescent protein expressing *S.* Typhimurium WT strain GPM2010 or *ΔsodCI sodCII* strain GPM2012 as described. The cells were counterstained with DAPI and were mounted with anti-fade diamond medium (Life Technology). Images were collected on a Leica SP5 inverted confocal microscope with a motorized stage and analyzed with the Fiji software package (40).

Murine infections

Bacteria were cultured overnight in LB medium at 37°C and diluted in sterile PBS. For competition assays selected strains of *S.* Typhimurium were mixed at a 1:1 ratio. Perforin-2 WT and KO 129X1/SvJ mice were inoculated by intraperitoneal injection. The CFU of each inoculum was quantified by plating and ranged from 500 to 1,000 total CFUs. Spleens and livers were collected four days after inoculation, and then homogenized (Omni International Tulsa) in 500 μl PBST (PBS, 0.1% Tween-20). Homogenates were diluted in sterile PBS and plated in triplicate on LB agar with antibiotic selection as appropriate for each strain in the initial inoculum. For each spleen and liver, mean CFUs were used to calculate competitive indices (CI) according to the following formula: CI = (strain A recovered / strain B recovered) / (strain A inoculum / strain B inoculum).

Statistical analyses

Statistical analyses were performed with GraphPad Prism 7 software. P values ≤ 0.05 were considered statistically significant and were determined by two-way ANOVA with Sidack's multiple comparisons test or one-way ANOVA with Tukey's multiple comparisons test.

Results

Perforin-2 limits the survival of phagocytosed bacteria independent of ROS

Because the interactions between *Salmonella* sp. and macrophages have been extensively characterized, we chose to exploit the *Salmonella*/phagocyte paradigm to probe the mechanism of Perforin-2 dependent killing of phagocytosed bacteria (41). Accordingly, PEMs and neutrophils isolated from WT and Perforin-2 KO mice were infected with *S.* Typhimurium. As expected from previous studies that have shown *Salmonella* survives within macrophages, the intracellular load of bacteria either increased or remained nearly constant in WT phagocytes (Fig. 1AB). However, Perforin-2 deficient phagocytes had significantly higher intracellular loads of *S.* Typhimurium than WT phagocytes (Fig. 1AB). This demonstrates that Perforin-2 limits the survival and/or replication of phagocytosed *S.* Typhimurium and is consistent with previous studies that have shown Perforin-2 is a potent

antimicrobial effector against *Salmonella* as well as gram-positive and acid-fast bacteria (24–26, 42).

One of the aforementioned studies also investigated the relationship between ROS and Perforin-2 and concluded that the bactericidal activity of ROS was dependent upon Perforin-2 (25). This was based on two principle findings. First, chemical inhibition of ROS production significantly enhanced the survival of phagocytosed *S.* Typhimurium –relative to mock treated cells– in WT but not Perforin-2 deficient PEMs. Second, WT PEMs killed a Δ*sodCI* strain of *S.* Typhimurium much more efficiently than WT *S.* Typhimurium. SodCI is a periplasmic superoxide dismutase that neutralizes ROS and thus promotes the survival of *S.* Typhimurium within phagosomes (25, 43). However, the *sodCI* mutant was found to be no less fit than the WT strain when Perforin-2 KO PEMs were used. Thus, both a chemical and genetic analysis suggest that ROS is not a significant bactericidal effector when Perforin-2 is absent.

As with the previous study we observed similar effects with both PEMs and neutrophils. In either case the *S.* Typhimurium *sodCI* mutant was efficiently killed by Peforin-2 proficient but not deficient phagocytes (Fig. 1CD). The source of phagocytic ROS is the multisubunit NADPH oxidase NOX2 (44). Assembly of the enzymatic complex involves the translocation of cytosolic proteins to the endosomal membrane to form the active complex that generates the respiratory burst (44). Likewise Perforin-2, a transmembrane protein of cytosolic vesicles, dynamically translocates to and fuses with phagocytic vesicles containing bacteria (24, 25). This raised the possibility that Perforin-2 is involved in the assembly and/or activation of the NADPH oxidase. If true the respiratory burst would be deficient in Perforin-2 KO phagocytes and would account for the survival of *S.* Typhimurium *sodCI* mutants in Perforin-2 deficient phagocytes.

To determine whether or not Perforin-2 is required for ROS production a luminol based chemiluminescence assay was used to quantify ROS productions in IFN-γ primed PEMs, peritoneal macrophages isolated without thioglycollate stimulation, and neutrophils from WT and Perforin-2 KO mice. We found that total ROS production was equally robust in WT and Perforin-2 KO macrophages that were stimulated with PMA or LPS (Fig. 2AB). The kinetics of ROS production was also similar as macrophages of both genotypes exhibited peak ROS production at 60 min. To confirm that the chemiluminescent signal was due to ROS production by a NADPH oxidase, phagocytes were pretreated with DPI; an inhibitor of NAPDH oxidases. As expected DPI treated cells produced negligible amounts of ROS (Fig. 2). Likewise, ROS production was also negligible in unstimulated macrophages (data not shown). As with macrophages, we found few statistically significant differences between total ROS production in WT and Perforin-2 KO neutrophils (Fig. 2CD). As was the case for total ROS, phagocytic ROS production was similar in both WT and Perforin-2 KO neutrophils (Fig. 2E). Although the signal was too low for us to quantify phagocytic ROS production in macrophages, we note that bacterial superoxide dismutases promote the survival of phagocytosed *S.* typhimurium in WT and Peforin-2 KO PEMs (Figs. 1 and 3). This indicates that both types of PEMs produce bactericidal levels of phagocytic ROS. Thus, we conclude that impaired ROS production cannot account for the survival of *S.* Typhimurium Δ*sodCI* mutants in Perforin-2 KO phagocytes.

SodCI and SodCII are functionally redundant in Perforin-2 KO phagocytes

Having excluded the possibility that Perforin-2 deficiency results in impaired ROS production, we next considered the possibility that *S.* Typhimurium *sodCI* mutants are resistant to ROS in Perforin-2 deficient but not proficient phagocytes. As the genome of *S.* Typhimurium encodes a second periplasmic superoxide dismutase (SodCII) we considered the possibility that it provides resistance to ROS in Perforin-2 KO phagocytes even though previous studies have concluded that SodCII does not attenuate ROS toxicity in WT cells and animals (11, 43). To determine whether or not SodCI and SodCII are functionally redundant we infected Perforin-2 proficient and deficient phagocytes with a *sodCI sodCII* double mutant. Unlike the Δ*sodCI sodCII*$^{+}$ strain which was killed by WT but not Perforin-2 KO phagocytes (Fig. 1CD), the Δ*sodCI sodCII::kan* strain was killed by both Perforin-2 WT and KO phagocytes (Fig. 3AB). Complementation of the double mutant with *sodCII* allowed the complemented strain to proliferate in Perforin-2 KO but not WT phagocytes (Fig. 3CD). Consistent with our findings that ROS production is similar in both WT and Perforin-2 deficient phagocytes (Fig. 2), DPI inhibition of NADPH oxidase allowed the *Salmonella* double mutant to proliferate in both Perforin-2 WT and KO PEMs (Fig. 4C). Likewise, both WT *Salmonella* and the *sodCI* mutant reached higher cellular loads in DPI treated PEMs than in untreated PEMs (Fig. 4). Thus, in agreement with previous studies (43, 45) we conclude that SodCII does not protect against ROS in WT phagocytes. However, the nullification of SodCII is clearly dependent upon Perforin-2 because SodCII is able to protect phagocytosed *S.* Typhimurium from the bactericidal effects of ROS in Perforin-2 KO phagocytes.

Perforin-2 facilitates the degradation of antigens enclosed within the bacterial envelope

Although SodCI and SodCII have similar enzymatic properties, only SodCI provides resistance to endosomal ROS in WT phagocytes (43). Studies by the Slauch laboratory have shown that this phenomenon is not the result of differential expression (43). Rather it is due to differential degradation of the two superoxide dismutases; SodCI is protease resistant while SodCII is protease sensitive (11, 43, 45). Thus, SodCII does not protect phagocytosed *S.* Typhimurium because it is proteolytically degraded. However we have found that SodCII is functional in Perforin-2 KO phagocytes (Fig. 3). Therefore, we considered it possible that the degradation of SodCII is Perforin-2 dependent. To determine whether or not this is the case we infected WT and KO PEMs with a strain of *S.* Typhimurium expressing SodCII-FLAG so that we could track the persistence of SodCII in the periplasm with a monoclonal antibody against the FLAG epitope. We also used antibodies against DnaK and flagellin to monitor the abundance of cytoplasmic and surface antigens respectively. Western blots of intracellular bacteria recovered 18 hours after infection revealed that extracellular flagellin, which was abundant on the surface of the bacteria prior to phagocytosis, was efficiently degraded in both WT and KO PEMs (Fig. 5A). In contrast there was a clear difference in the abundance of SodCII in bacteria recovered from Perforin-2 KO and WT PEMs (Fig. 5A). We acknowledge that the lack of suitable antibodies against SodCII prevents us from determining by Western blot if the loss of the SodCII signal is the result of the complete destruction of SodCII or merely clipping of the FLAG epitope. However, our in vitro data is consistent with Perforin-2 dependent destruction of SodCII because SodCII confers a protective phenotype in Perforin-2 KO but not WT phagocytes and animals (Fig. 3 and

below). Moreover, the apparent Perforin-2 dependent destruction of SodCII was not due to differences in bacterial load because the difference in SodCII abundance was statistically significant when experimental replicates were quantified and normalized to DnaK of the bacterial cytoplasm (Fig. 5B). A further indication that the bacterial loads were similar in these experiments is the fact that the difference in the amount of DnaK normalized to host β-actin was insignificant while the difference in the amount of SodCII normalized to β-actin was significant (Fig. 5B).

We also examined the degradation of the three bacterial antigens at earlier time points. Because these experiments required significantly more phagocytes we used BMDM which can be obtained at higher yields than PEMs. As with PEMs extracellular flagellin was efficiently degraded in both WT and Perforin-2 KO BMDM (Fig. 5C). There was also apparent degradation of both SodCII and DnaK in both types of cells. Nevertheless there was less SodCII in bacteria recovered from WT than KO phagocytes. This difference was statistically significant at 3 and 6 hours when normalized to DnaK even though concurrent degradation of DnaK likely results in an underestimation of the difference (Fig. 5D). The degradation of DnaK also appears to lag that of SodCII; although, it is unclear if this is due to differences in protease accessibility and/or susceptibility. Differences in expression may also contribute to the apparent differences in degradation rates of SodCII compared to DnaK. Relative to β-actin the differences in SodCII in WT compared to Perforin-2 KO BMDM was significant even at the 1 hour time point. This cannot be due to higher loads of the bacteria in Perforin-2 KO phagocytes because the amount of DnaK normalized to β-actin also decreased over time; even in KO cells. Additionally, extrapolation of our PEMs bactericidal assays suggest the differences in bacterial loads is likely to be negligible at early time points; especially, at 1 hour.

In aggregate our results demonstrate that Perforin-2 facilitates the degradation of internal – but not extracellular– antigens of phagocytosed bacteria. This is not due to differences in the acidification of SCVs, which could affect protease activity, because the acidification profiles of SCVs in WT and Perforin-2 KO PEMs were found to be similar (Supplemental Fig. S1). Rather it most likely involves a direct interaction between Perforin-2 and the bacterial envelope; because, as a type I transmembrane protein the putative pore forming MACPF domain of Perforin-2 would be located inside the vacuole with the bacteria. Moreover, Perforin-2 has been shown to colocalize with phagocytosed WT *S.* Typhimurium (25). The rapid formation of intracellular punctate bodies containing Perforin-2 –which is triggered by PAMPs and an indication of Perforin-2 trafficking (24)– was similar when RAW264.7 cells expressing Perforin-2-E2-Crimson were infected with either WT *S.* Typhimurium or *sodCI sodCII* double mutant (Supplemental Fig. S2). Although there was no *a priori* reason to suspect that the presence or absence of bacterial superoxide dismutases would affect the intracellular trafficking of Perforin-2, the latter results further support a model in which Perforin-2 attacks the envelope of phagocytosed bacteria.

Perforin-2 negates SodCII in vivo

Having established that Perforin-2 facilitates the degradation of SodCII in vitro, the relevance of our observations were evaluated in a murine infection model. In brief, WT and

Perforin-2 KO mice were inoculated intraperitoneally with a mixture of WT *S.* Typhimurium and a *sodCI* mutant at a 1:1 ratio. Four days after infection liver and spleen homogenates were plated on selective media to enumerate the load of each strain. Consistent with previous studies fewer *sodCI::kan* bacteria were recovered than WT bacteria recovered from Perforin-2 WT mice. The derived CI were accordingly low and demonstrate that the *sodCI* mutant is significantly attenuated in Perforin-2 proficient mice (Fig. 6A). In contrast, there was little to no attenuation of the *sodCI::kan* strain in Perforin-2 KO mice as indicated by CI near or at 1.0 (Fig. 6A). Similar results were obtained with a strain of *S.* Typhimurium that had spontaneously lost the pSLT virulence plasmid (Fig. 6B) (46). Thus, SodCI is not essential in the absence of Perforin-2.

Based on our in vitro studies the persistence of SodCII was the most likely explanation for the lack of attenuation of the *sodCI* mutant in Perforin-2 KO mice. Indeed this was found to be the case because a *sodCI sodCII* double mutant was found to be significantly attenuated relative to WT bacteria in Perforin-2 KO mice (Fig. 6C). Furthermore, complementation of the *sodCI sodCII* double mutant with *sodCII* resulted in a strain that was as virulent as WT *S.* Typhimurium in Perforin-2 KO mice (Fig. 6D). In fact there appeared to be a slight competitive advantage of the complemented strain over the WT strain as indicated by competitive indices > 1. This could be the result of higher expression levels of *sodCII* from a heterologous promoter in our construct. In contrast, complementation with *sodCII* failed to rescue the double mutant in WT mice (Fig. 6D). In aggregate our in vivo studies demonstrate that SodCII confers a protective advantage in Perforin-2 KO but not WT mice. As such they are consistent with our in vitro finding that Perforin-2 facilitates the degradation of SodCII.

Discussion

Perforin-2 is a type I transmembrane protein that we have previously shown localizes to endosomal vesicles as well as the endoplasmic reticulum, Golgi, and plasma membrane (25). A separate study that focused on the proteome of endocytic vesicles also found that Perforin-2 is present in endosomes following phagocytosis of latex beads by J774 macrophages (47). The same study also found that Perforin-2 was more abundant in late endosomes and lysosomes than early endosomes. Perforin-2 is also coincident with subunits of the phagocytic NAPDH oxidase, proton transporters, and many other antimicrobial effectors of phagosomes and/or the phagolysosomes (47, 48). LPS stimulation of BMDM has also been shown to increase the abundance of Perforin-2 in endolysosomes compared to untreated cells (48). This is consistent with our own studies in which we reported that LPS results in the accumulation of Perforin-2 in vesicular structures and that Perforin-2 colocalizes with phagocytosed bacteria such as *Escherichia coli* and *S.* Typhimurium (24, 25). In aggregate these studies demonstrate that the subcellular distribution of Perforin-2 is consistent with its ability to facilitate the destruction of phagocytosed bacteria.

Although most phagocytosed bacteria are rapidly killed some are able to resist phagocytic antimicrobials and even survive within professional phagocytes. The latter includes *S.* Typhimurium which must survive the respiratory burst and other antimicrobial assaults prior to the formation of SCVs; specialized niches within macrophages that afford the pathogen a

more favorable environment than phagosomes or phagolysosomes (49). A central player in the survival of the respiratory burst is SodCI; a periplasmic superoxide dismutase that converts superoxide to hydrogen peroxide which is subsequently detoxified by bacterial catalases and peroxidases (50–53). The pivotal role of SodCI in protecting *Salmonella* from ROS has been confirmed by several studies that have shown that *sodCI* mutants are more susceptible to ROS killing in vitro and less virulent than WT *Salmonella* in vivo (43, 45, 54, 55). However we have found that a *sodCI* null mutant is able to proliferate in Perforin-2 deficient phagocytes. Moreover the *sodCI* null mutant is as virulent as WT *S.* Typhimurium in Perforin-2 deficient –but not proficient– mice. Because we have found that the production of phagocytic ROS is independent of Perforin-2, the survival of the *sodCI* mutant is not due to differences in ROS production. Rather it is due to the persistence of SodCII, a second periplasmic superoxide dismutase, in Perforin-2 deficient phagocytes. Consistent with our in vitro results we have also found that SodCI and SodCII are functionally redundant in Perforin-2 KO mice.

The persistence of SodCII was unexpected because previous studies have shown that it is normally degraded by proteases of the phagolysosome (43, 45). In contrast SodCI is resistant to proteolytic degradation and thus provides resistance to ROS in the phagolysosome (43). Our results in Perforin-2 WT cells and animals are consistent with these latter studies because *sodCII* is unable to complement a *sodCI sodCII* double mutant. However, *sodCII* is able to complement the double mutant in Perforin-2 KO animals and isolated phagocytes. Thus, the presence of Perforin-2 is associated with the inactivation of SodCII.

How does Perforin-2 inactivate SodCII? Consistent with previous studies we have shown that SodCII is proteolytically degraded in the phagosome and/or phagolysosome in Perforin-2 proficient cells (43, 45). However, the degradation of SodCII is significantly attenuated in phagocytes lacking Perforin-2. Similar results were observed with cytoplasmic DnaK in BMDM. This was not due to a general defect in protease activity in the phagolysosome because the surface antigen flagellin was degraded whether or not Perforin-2 was present. Thus, Perforin-2 facilitates the degradation of antigens contained within the envelope of phagocytosed bacteria. However, it is unlikely that Perforin-2 is itself a protease because it lacks significant homology to a known protease or protease motif. What Perforin-2 does have is a MACPF domain (Fig. 7) (56–58). This suggest that Perforin-2 is a pore forming protein and putative Perforin-2 pores have been imaged by transmission electron microscopy (25). However to date it has not been possible to confirm that the imaged structures contain Perforin-2 due to the absence of suitable antibodies. Nor has it been confirmed that the structures are in fact pores. However, other MACPF containing proteins such as complement protein C9 and Perforin have been shown to polymerize and form pores in lipid membranes (17, 20, 22, 59, 60). For example, 22 monomers of C9 polymerize to form a pore in the outer membrane of gram-negative bacteria with an inner diameter of 120 Å (22, 59, 61). Because Perforin-2 is a type I transmembrane protein with its membrane spanning alpha helix near its carboxy-terminus, the MACPF domain of Perforin-2 would reside in the lumen of endosomes and phagosomes. In this orientation its MACPF domain would reside in the same compartment as phagocytosed bacteria. Thus, we propose that Perforin-2 polymerizes – perhaps after cleavage from its transmembrane

domain by a lysosomal protease– and forms pores in the envelope of phagocytosed bacteria (Fig. 7). This model is consistent with our experimental observations with *S.* Typhimurium since the protease that degrades SodCII would enter the periplasmic space through poly-Perforin-2 pores. Because SodCII is not anchored in the periplasm, it may also diffuse through the pore and be degraded in the lumen of the phagosome (11, 43, 45). In either case SodCII is able to persist in the periplasm and protect the bacterium from the bactericidal effects of ROS when Perforin-2 is absent.

In addition to Perforin-2 there is evidence that the cathelicidins CRAMP and LL-37 also play a role in disrupting the envelope of phagocytosed gram-negative bacteria in murine and human macrophages respectively (11–14). Of particular relevance to this study are previous studies that have shown that CRAMP is active against phagocytosed *S.* Typhimurium (11, 12). In one it was shown that CRAMP inhibits the division of *S.* Typhimurium. The result was filamentous bacteria and it was further shown that filamentation was protease dependent (12). In another study it was shown that CRAMP is associated with the loss of SodCII from the periplasm of *S.* Typhimurium in vitro (11). Moreover SodCII promoted the survival of *S.* Typhimurium in CRAMP deficient but not proficient mice. However in the latter study the authors also noted that the loss of CRAMP failed to fully abolish the degradation of SodCII. Our study suggest that this is most likely due to the activity of Perforin-2. Although it is clear that Perforin-2 and cathelicidins can act independently of one another, it remains to be determined if they also act synergistically. In the case of gram-negative bacteria a particularly intriguing model is the possibility that Perforin-2 forms a conduit in the outer membrane through which cathelicidin or other antimicrobial peptides transit to reach the bacterial inner membrane. Alternatively the deployment of independent mechanisms to disrupt the envelope of phagocytosed bacteria may be an insurance strategy against pathogen resistance to any particular mechanism.

Supplementary Material

Refer to Web version on PubMed Central for supplementary material.

Acknowledgments

Research reported in this publication was supported by Grant Number AI110810 from the National Institute of Allergy and Infectious Diseases of the National Institutes of Health (NIAID NIH). Its contents are solely the responsibility of the authors and do not necessarily represent the official views of the NIH.

Abbreviations:

ROS
reactive oxygen species

MACPF
membrane attack complex perforin

PEMs
peritoneal exudate macrophages

BMDM
bone marrow derived macrophage

DPI
diphenyleneiodonium chloride

WT
wild-type

KO
knockout

S.
Typhimurium

Salmonella enterica serovar
Typhimurium

LB
Luria-Bertani

CI
competitive indices

CRAMP
cathelicidin-related antimicrobial peptide

SCVs
Salmonella containing vacuoles

References

1. Karimi G, Houee Levin C, Dagher MC, Baciou L, and Bizouarn T. 2014 Assembly of phagocyte NADPH oxidase: A concerted binding process? Biochimica et biophysica acta 1840: 3277–3283. [PubMed: 25108064]
2. Nauseef WM 2004 Assembly of the phagocyte NADPH oxidase. Histochemistry and cell biology 122: 277–291. [PubMed: 15293055]
3. Cederlund A, Gudmundsson GH, and Agerberth B. 2011 Antimicrobial peptides important in innate immunity. The FEBS journal 278: 3942–3951. [PubMed: 21848912]
4. Ellison RT, 3rd, and Giehl TJ. 1991 Killing of gram-negative bacteria by lactoferrin and lysozyme. The Journal of clinical investigation 88: 1080–1091. [PubMed: 1918365]
5. Martinez RJ, and Carroll SF. 1980 Sequential metabolic expressions of the lethal process in human serum-treated Escherichia coli: role of lysozyme. Infection and immunity 28: 735–745. [PubMed: 6156906]
6. Gallo RL, Kim KJ, Bernfield M, Kozak CA, Zanetti M, Merluzzi L, and Gennaro R. 1997 Identification of CRAMP, a cathelin-related antimicrobial peptide expressed in the embryonic and adult mouse. The Journal of biological chemistry 272: 13088–13093. [PubMed: 9148921]
7. Turner J, Cho Y, Dinh NN, Waring AJ, and Lehrer RI. 1998 Activities of LL-37, a cathelin-associated antimicrobial peptide of human neutrophils. Antimicrobial agents and chemotherapy 42: 2206–2214. [PubMed: 9736536]

8. Wiesner J, and Vilcinskas A. 2010 Antimicrobial peptides: the ancient arm of the human immune system. Virulence 1: 440–464. [PubMed: 21178486]
9. Zanetti M 2004 Cathelicidins, multifunctional peptides of the innate immunity. Journal of leukocyte biology 75: 39–48. [PubMed: 12960280]
10. Henzler Wildman KA, Lee DK, and Ramamoorthy A. 2003 Mechanism of lipid bilayer disruption by the human antimicrobial peptide, LL-37. Biochemistry 42: 6545–6558. [PubMed: 12767238]
11. Kim B, Richards SM, Gunn JS, and Slauch JM. 2010 Protecting against antimicrobial effectors in the phagosome allows SodCII to contribute to virulence in Salmonella enterica serovar Typhimurium. Journal of bacteriology 192: 2140–2149. [PubMed: 20154132]
12. Rosenberger CM, Gallo RL, and Finlay BB. 2004 Interplay between antibacterial effectors: a macrophage antimicrobial peptide impairs intracellular Salmonella replication. Proceedings of the National Academy of Sciences of the United States of America 101: 2422–2427. [PubMed: 14983025]
13. Sonawane A, Santos JC, Mishra BB, Jena P, Progida C, Sorensen OE, Gallo R, Appelberg R, and Griffiths G. 2011 Cathelicidin is involved in the intracellular killing of mycobacteria in macrophages. Cellular microbiology 13: 1601–1617. [PubMed: 21790937]
14. Stephan A, Batinica M, Steiger J, Hartmann P, Zaucke F, Bloch W, and Fabri M. 2016 LL37:DNA complexes provide antimicrobial activity against intracellular bacteria in human macrophages. Immunology 148: 420–432. [PubMed: 27177697]
15. Spilsbury K, O'Mara MA, Wu WM, Rowe PB, Symonds G, and Takayama Y. 1995 Isolation of a novel macrophage-specific gene by differential cDNA analysis. Blood 85: 1620–1629. [PubMed: 7888681]
16. Gudmundsson GH, Agerberth B, Odeberg J, Bergman T, Olsson B, and Salcedo R. 1996 The human gene FALL39 and processing of the cathelin precursor to the antibacterial peptide LL-37 in granulocytes. European journal of biochemistry 238: 325–332. [PubMed: 8681941]
17. Law RH, Lukoyanova N, Voskoboinik I, Caradoc-Davies TT, Baran K, Dunstone MA, D'Angelo ME, Orlova EV, Coulibaly F, Verschoor S, Browne KA, Ciccone A, Kuiper MJ, Bird PI, Trapani JA, Saibil HR, and Whisstock JC. 2010 The structural basis for membrane binding and pore formation by lymphocyte perforin. Nature 468: 447–451. [PubMed: 21037563]
18. Voskoboinik I, Whisstock JC, and Trapani JA. 2015 Perforin and granzymes: function, dysfunction and human pathology. Nat Rev Immunol 15: 388–400. [PubMed: 25998963]
19. Lichtenheld MG, Olsen KJ, Lu P, Lowrey DM, Hameed A, Hengartner H, and Podack ER. 1988 Structure and function of human perforin. Nature 335: 448–451. [PubMed: 3419519]
20. Podack ER, Olsen KJ, Lowrey DM, and Lichtenheld M. 1989 Structure and function of perforin. Curr Top Microbiol Immunol 140: 11–17. [PubMed: 2644072]
21. Thiery J, Keefe D, Boulant S, Boucrot E, Walch M, Martinvalet D, Goping IS, Bleackley RC, Kirchhausen T, and Lieberman J. 2011 Perforin pores in the endosomal membrane trigger the release of endocytosed granzyme B into the cytosol of target cells. Nat Immunol 12: 770–777. [PubMed: 21685908]
22. Dudkina NV, Spicer BA, Reboul CF, Conroy PJ, Lukoyanova N, Elmlund H, Law RH, Ekkel SM, Kondos SC, Goode RJ, Ramm G, Whisstock JC, Saibil HR, and Dunstone MA. 2016 Structure of the poly-C9 component of the complement membrane attack complex. Nature communications 7: 10588.
23. McCormack R, de Armas LR, Shiratsuchi M, Ramos JE, and Podack ER. 2013 Inhibition of intracellular bacterial replication in fibroblasts is dependent on the perforin-like protein (perforin-2) encoded by macrophage-expressed gene 1. Journal of innate immunity 5: 185–194. [PubMed: 23257510]
24. McCormack RM, Lyapichev K, Olsson ML, Podack ER, and Munson GP. 2015 Enteric pathogens deploy cell cycle inhibiting factors to block the bactericidal activity of Perforin-2. eLife 4.
25. McCormack RM, de Armas LR, Shiratsuchi M, Fiorentino DG, Olsson ML, Lichtenheld MG, Morales A, Lyapichev K, Gonzalez LE, Strbo N, Sukumar N, Stojadinovic O, Plano GV, Munson GP, Tomic-Canic M, Kirsner RS, Russell DG, and Podack ER. 2015 Perforin-2 is essential for intracellular defense of parenchymal cells and phagocytes against pathogenic bacteria. eLife 4.

26. McCormack R, Bahnan W, Shrestha N, Boucher J, Barreto M, Barrera CM, Dauer EA, Freitag NE, Khan WN, Podack ER, and Schesser K. 2016 Perforin-2 Protects Host Cells and Mice by Restricting the Vacuole to Cytosol Transitioning of a Bacterial Pathogen. Infection and immunity 84: 1083–1091. [PubMed: 26831467]
27. Benard EL, Racz PI, Rougeot J, Nezhinsky AE, Verbeek FJ, Spaink HP, and Meijer AH. 2015 Macrophage-expressed perforins mpeg1 and mpeg1.2 have an anti-bacterial function in zebrafish. Journal of innate immunity 7: 136–152. [PubMed: 25247677]
28. Nikaido H, Levinthal M, Nikaido K, and Nakane K. 1967 Extended deletions in the histidine-rough-B region of the Salmonella chromosome. Proceedings of the National Academy of Sciences of the United States of America 57: 1825–1832. [PubMed: 5231414]
29. Datsenko KA, and Wanner BL. 2000 One-step inactivation of chromosomal genes in Escherichia coli K-12 using PCR products. Proceedings of the National Academy of Sciences of the United States of America 97: 6640–6645. [PubMed: 10829079]
30. Haldimann A, and Wanner BL. 2001 Conditional-replication, integration, excision, and retrieval plasmid-host systems for gene structure-function studies of bacteria. Journal of bacteriology 183: 6384–6393. [PubMed: 11591683]
31. Uzzau S, Figueroa-Bossi N, Rubino S, and Bossi L. 2001 Epitope tagging of chromosomal genes in Salmonella. Proceedings of the National Academy of Sciences of the United States of America 98: 15264–15269. [PubMed: 11742086]
32. Amann E, Ochs B, and Abel KJ. 1988 Tightly regulated tac promoter vectors useful for the expression of unfused and fused proteins in Escherichia coli. Gene 69: 301–315. [PubMed: 3069586]
33. Zhang X, Goncalves R, and Mosser DM. 2008 The isolation and characterization of murine macrophages. Current protocols in immunology Chapter 14: Unit 14 11.
34. Nathan CF, and Root RK. 1977 Hydrogen peroxide release from mouse peritoneal macrophages: dependence on sequential activation and triggering. The Journal of experimental medicine 146: 1648–1662. [PubMed: 925614]
35. Luo Y, and Dorf ME. 2001 Isolation of mouse neutrophils. Current protocols in immunology Chapter 3: Unit 3 20.
36. Lutwyche P, Cordeiro C, Wiseman DJ, St-Louis M, Uh M, Hope MJ, Webb MS, and Finlay BB. 1998 Intracellular delivery and antibacterial activity of gentamicin encapsulated in pH-sensitive liposomes. Antimicrobial agents and chemotherapy 42: 2511–2520. [PubMed: 9756749]
37. Laroux FS, Romero X, Wetzler L, Engel P, and Terhorst C. 2005 Cutting edge: MyD88 controls phagocyte NADPH oxidase function and killing of gram-negative bacteria. Journal of immunology 175: 5596–5600.
38. Yamazaki T, Kawai C, Yamauchi A, and Kuribayashi F. 2011 A highly sensitive chemiluminescence assay for superoxide detection and chronic granulomatous disease diagnosis. Tropical medicine and health 39: 41–45. [PubMed: 22028609]
39. Drecktrah D, Knodler LA, Ireland R, and Steele-Mortimer O. 2006 The mechanism of Salmonella entry determines the vacuolar environment and intracellular gene expression. Traffic 7: 39–51. [PubMed: 16445685]
40. Schindelin J, Arganda-Carreras I, Frise E, Kaynig V, Longair M, Pietzsch T, Preibisch S, Rueden C, Saalfeld S, Schmid B, Tinevez JY, White DJ, Hartenstein V, Eliceiri K, Tomancak P, and Cardona A. 2012 Fiji: an open-source platform for biological-image analysis. Nat Methods 9: 676–682. [PubMed: 22743772]
41. Steele-Mortimer O 2008 The Salmonella-containing vacuole: moving with the times. Current opinion in microbiology 11: 38–45. [PubMed: 18304858]
42. Fields KA, McCormack R, de Armas LR, and Podack ER. 2013 Perforin-2 restricts growth of Chlamydia trachomatis in macrophages. Infection and immunity 81: 3045–3054. [PubMed: 23753625]
43. Krishnakumar R, Craig M, Imlay JA, and Slauch JM. 2004 Differences in enzymatic properties allow SodCI but not SodCII to contribute to virulence in Salmonella enterica serovar Typhimurium strain 14028. Journal of bacteriology 186: 5230–5238. [PubMed: 15292124]

44. Panday A, Sahoo MK, Osorio D, and Batra S. 2015 NADPH oxidases: an overview from structure to innate immunity-associated pathologies. Cellular & molecular immunology 12: 5–23. [PubMed: 25263488]
45. Krishnakumar R, Kim B, Mollo EA, Imlay JA, and Slauch JM. 2007 Structural properties of periplasmic SodCI that correlate with virulence in Salmonella enterica serovar Typhimurium. Journal of bacteriology 189: 4343–4352. [PubMed: 17416645]
46. McClelland M, Sanderson KE, Spieth J, Clifton SW, Latreille P, Courtney L, Porwollik S, Ali J, Dante M, Du F, Hou S, Layman D, Leonard S, Nguyen C, Scott K, Holmes A, Grewal N, Mulvaney E, Ryan E, Sun H, Florea L, Miller W, Stoneking T, Nhan M, Waterston R, and Wilson RK. 2001 Complete genome sequence of Salmonella enterica serovar Typhimurium LT2. Nature 413: 852–856. [PubMed: 11677609]
47. Duclos S, Clavarino G, Rousserie G, Goyette G, Boulais J, Camossetto V, Gatti E, LaBoissiere S, Pierre P, and Desjardins M. 2011 The endosomal proteome of macrophage and dendritic cells. Proteomics 11: 854–864. [PubMed: 21280226]
48. Nakamura N, Lill JR, Phung Q, Jiang Z, Bakalarski C, de Maziere A, Klumperman J, Schlatter M, Delamarre L, and Mellman I. 2014 Endosomes are specialized platforms for bacterial sensing and NOD2 signalling. Nature 509: 240–244. [PubMed: 24695226]
49. Anderson CJ, and Kendall MM. 2017 Salmonella enterica Serovar Typhimurium Strategies for Host Adaptation. Frontiers in microbiology 8: 1983. [PubMed: 29075247]
50. Aussel L, Zhao W, Hebrard M, Guilhon AA, Viala JP, Henri S, Chasson L, Gorvel JP, Barras F, and Meresse S. 2011 Salmonella detoxifying enzymes are sufficient to cope with the host oxidative burst. Molecular microbiology 80: 628–640. [PubMed: 21362067]
51. Hebrard M, Viala JP, Meresse S, Barras F, and Aussel L. 2009 Redundant hydrogen peroxide scavengers contribute to Salmonella virulence and oxidative stress resistance. Journal of bacteriology 191: 4605–4614. [PubMed: 19447905]
52. Slauch JM 2011 How does the oxidative burst of macrophages kill bacteria? Still an open question. Molecular microbiology 80: 580–583. [PubMed: 21375590]
53. Storz G, and Imlay JA. 1999 Oxidative stress. Current opinion in microbiology 2: 188–194. [PubMed: 10322176]
54. Craig M, and Slauch JM. 2009 Phagocytic superoxide specifically damages an extracytoplasmic target to inhibit or kill Salmonella. PloS one 4: e4975. [PubMed: 19305502]
55. Fang FC, DeGroote MA, Foster JW, Baumler AJ, Ochsner U, Testerman T, Bearson S, Giard JC, Xu Y, Campbell G, and Laessig T. 1999 Virulent Salmonella typhimurium has two periplasmic Cu, Zn-superoxide dismutases. Proceedings of the National Academy of Sciences of the United States of America 96: 7502–7507. [PubMed: 10377444]
56. McCormack R, and Podack ER. 2015 Perforin-2/Mpeg1 and other pore-forming proteins throughout evolution. Journal of leukocyte biology 98: 761–768. [PubMed: 26307549]
57. Podack ER, and Munson GP. 2016 Killing of Microbes and Cancer by the Immune System with Three Mammalian Pore-Forming Killer Proteins. Frontiers in immunology 7: 464. [PubMed: 27857713]
58. Ni T, and Gilbert RJC. 2017 Repurposing a pore: highly conserved perforin-like proteins with alternative mechanisms. Philos Trans R Soc Lond B Biol Sci 372.
59. Podack ER, Tschoop J, and Muller-Eberhard HJ. 1982 Molecular organization of C9 within the membrane attack complex of complement. Induction of circular C9 polymerization by the C5b-8 assembly. The Journal of experimental medicine 156: 268–282. [PubMed: 6177822]
60. Podack ER, and Tschopp J. 1982 Polymerization of the ninth component of complement (C9): formation of poly(C9) with a tubular ultrastructure resembling the membrane attack complex of complement. Proceedings of the National Academy of Sciences of the United States of America 79: 574–578. [PubMed: 6952208]
61. Tschopp J, and Podack ER. 1981 Membranolysis by the ninth component of human complement. Biochemical and biophysical research communications 100: 1409–1414. [PubMed: 7271808]

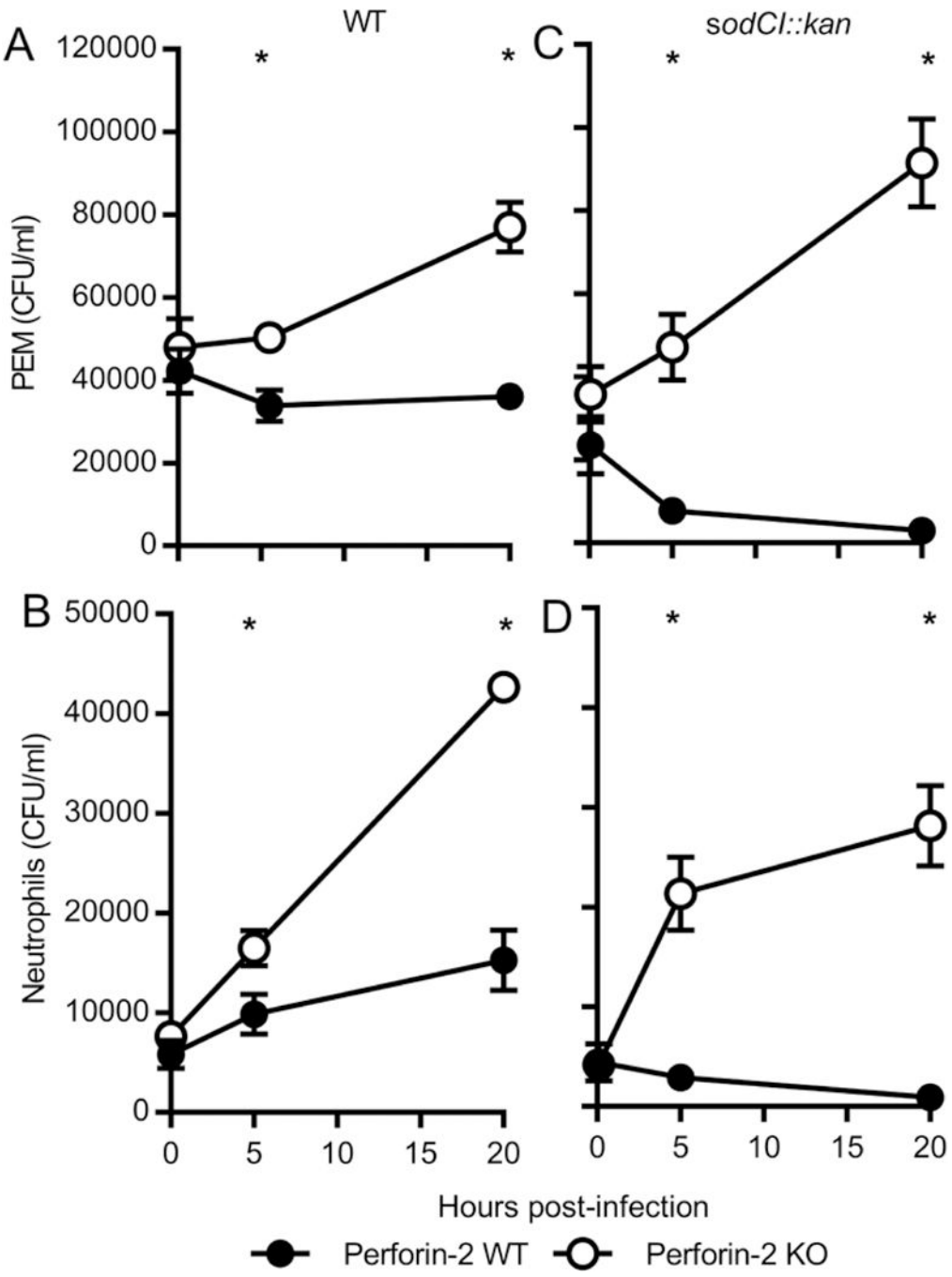

FIGURE 1.

Perforin-2 limits the survival of phagocytosed bacteria. As indicated PEM or peritoneal neutrophils were isolated from WT and Perforin-2 KO mice and stimulated with IFN-γ for 14 hours prior to infection with (AB) WT *S.* Typhimurium strain GPM2004, or (CD) strain ST188 [*sodCI::kan*]. Gentamicin was used to eliminate extracellular bacteria and intracellular bacteria were enumerated by plating cellular lysates. Means and standard deviations are shown; $n = 3$. Two-way ANOVA with Sidack's multiple comparisons test. $*P \leq 0.05$.

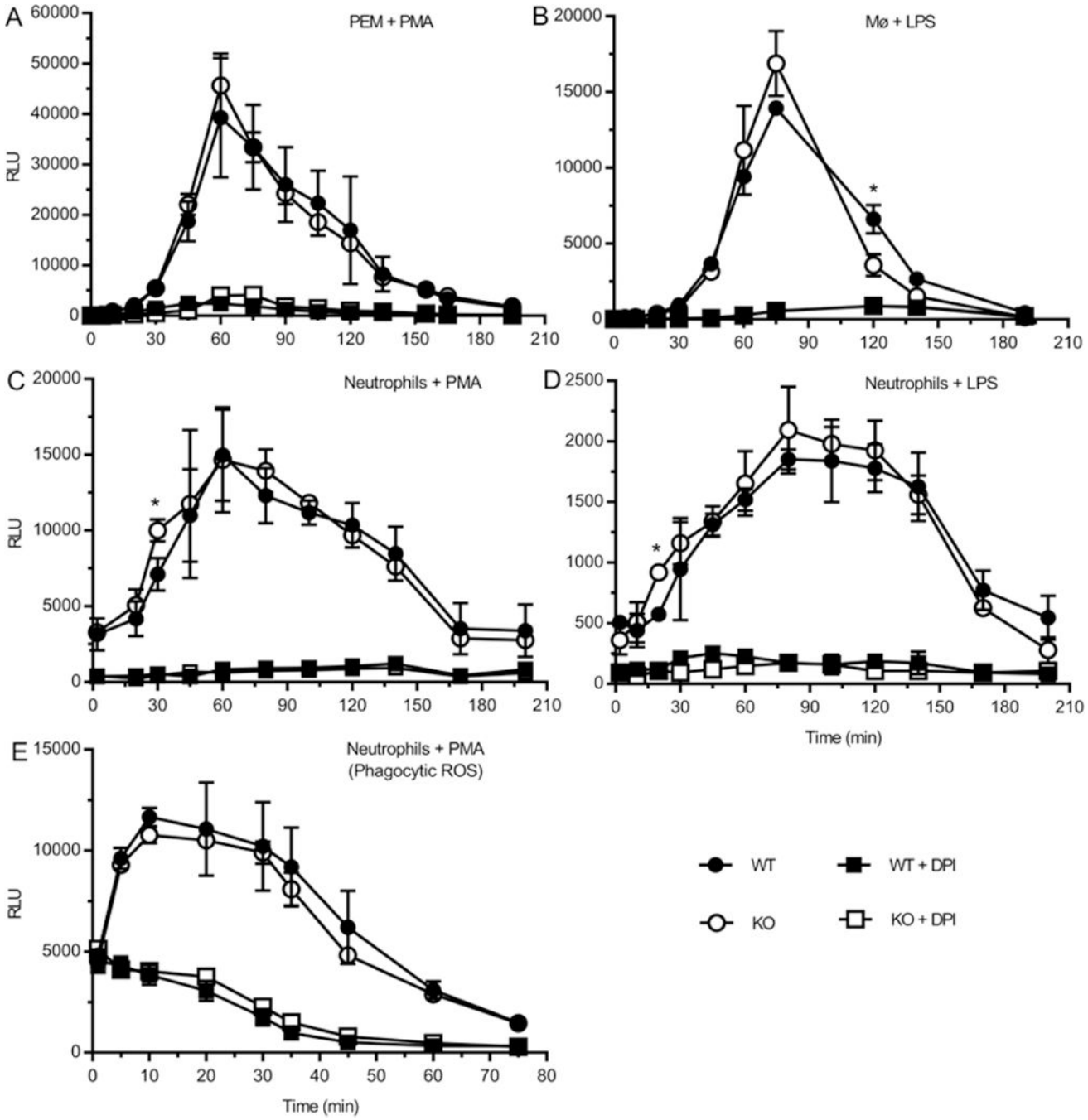

FIGURE 2.

Perforin-2 is not required for ROS production in phagocytes. As indicated WT and Perforin-2 -KO peritoneal (A,B) macrophages and (C,D) neutrophils were stimulated with PMA or LPS to elicit ROS production which was detected by luminal based chemiluminescence. (E) Phagocytic ROS production of Perforin-2 WT or KO neutrophils induced with PMA was detected after phagocytosis of luminal coupled beads. An enhancer was added to amplify chemiluminescence when macrophages were used. As indicated some cells were also treated with DPI, an inhibitor of the phagocytic NAPDH oxidase. ROS

activity is reported as mean relative light units (RLUs) ± SD; $n = 3$. Data were analyzed by two-way ANOVA with Sidack's multiple comparisons test. *$P \leq 0.05$.

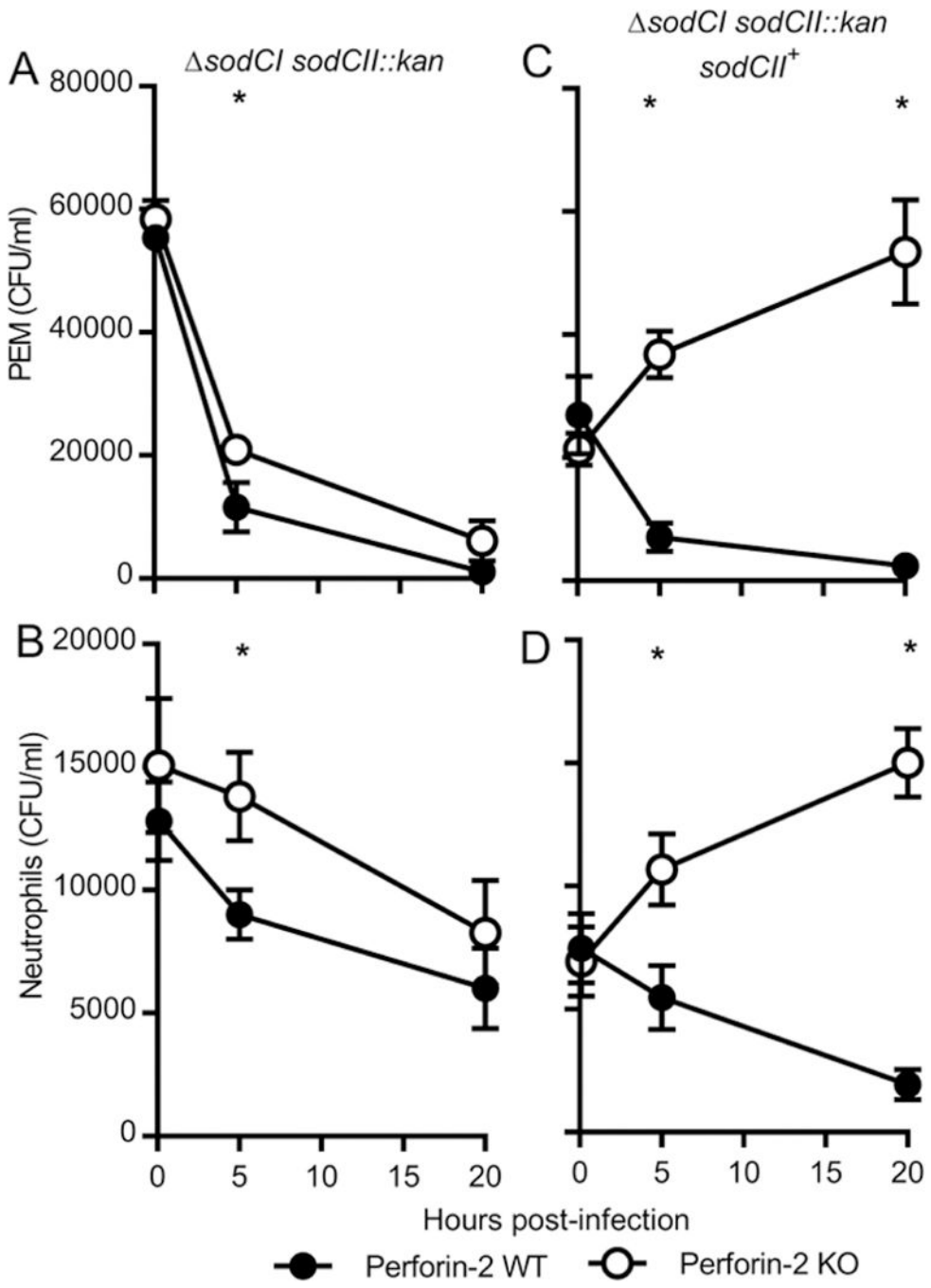

FIGURE 3.

SodCII is functional in the absence of Perforin-2. As indicated PEM or peritoneal neutrophils were isolated from WT and Perforin-2 KO mice and stimulated with IFN-γ for 14 hours prior to infection with *S.* Typhimurium strain (AB) ST189 [Δ*sodCI sodCII::kan*] or (CD) GPM2008 [Δ*sodCI sodCII::kan sodCII*$^{+}$]. Gentamicin was used to eliminate extracellular bacteria and intracellular bacteria were enumerated by plating cellular lysates. Means and standard deviations are shown; $n = 3$. Data were analyzed by two-way ANOVA with Sidack's multiple comparisons test. $*P \leq 0.05$.

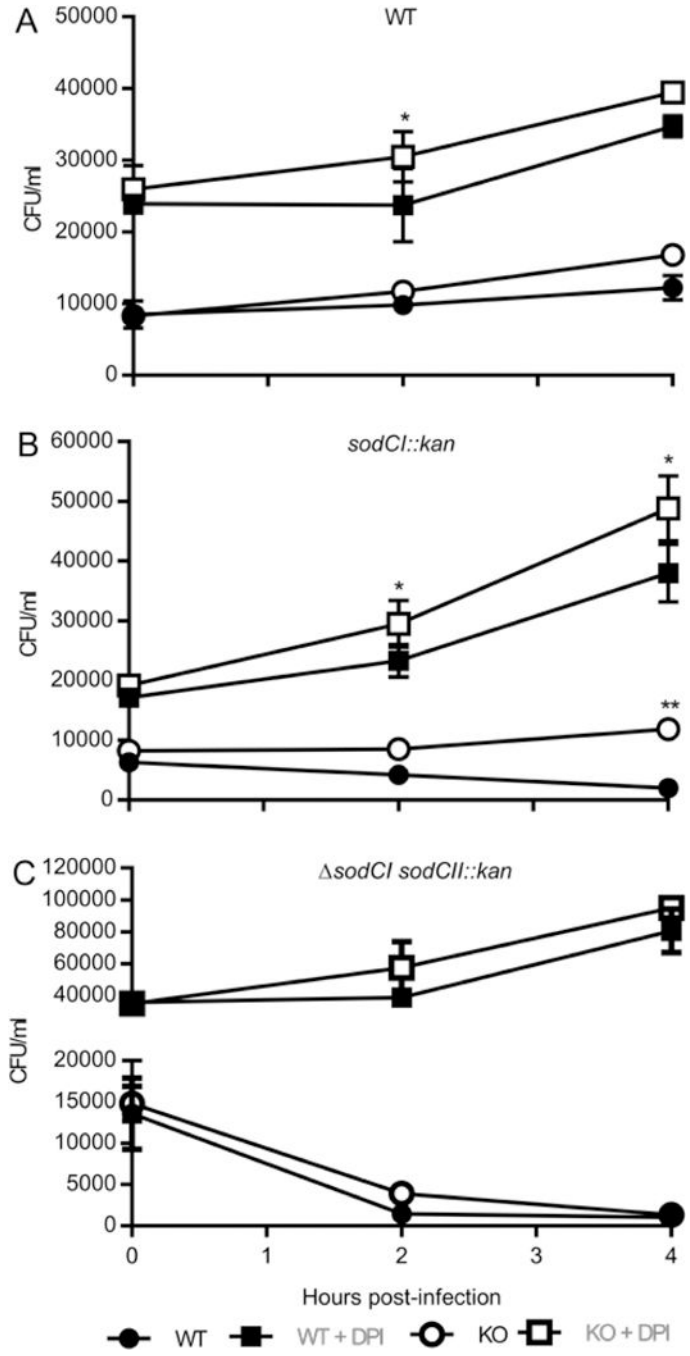

FIGURE 4.

Inhibition of ROS production allows *Salmonella* to proliferate intracellularly. PEMs from WT and Perforin-2 KO mice were stimulated with IFN-γ 14 h prior to infection. As indicated some cells were also treated with DPI 30 min before infection with (A) WT *S.* Typhimurium strain GPM2004, (B) strain ST188 [*sodCI::kan*] or (C) *S.* Typhimurium strain ST189 [Δ*sodCI sodCII::kan*]. Gentamicin was used to eliminate extracellular bacteria and intracellular bacteria were enumerated by plating cellular lysates. Means and standard deviations are shown; $n = 3$. Data were analyzed by two-way ANOVA with Sidack's

multiple comparisons test. * $P \leq 0.05$, comparison of DPI treated Perforin-2 WT and KO cells; ** $P \leq 0.05$, comparison of Perforin-2 WT and KO cells without DPI treatment

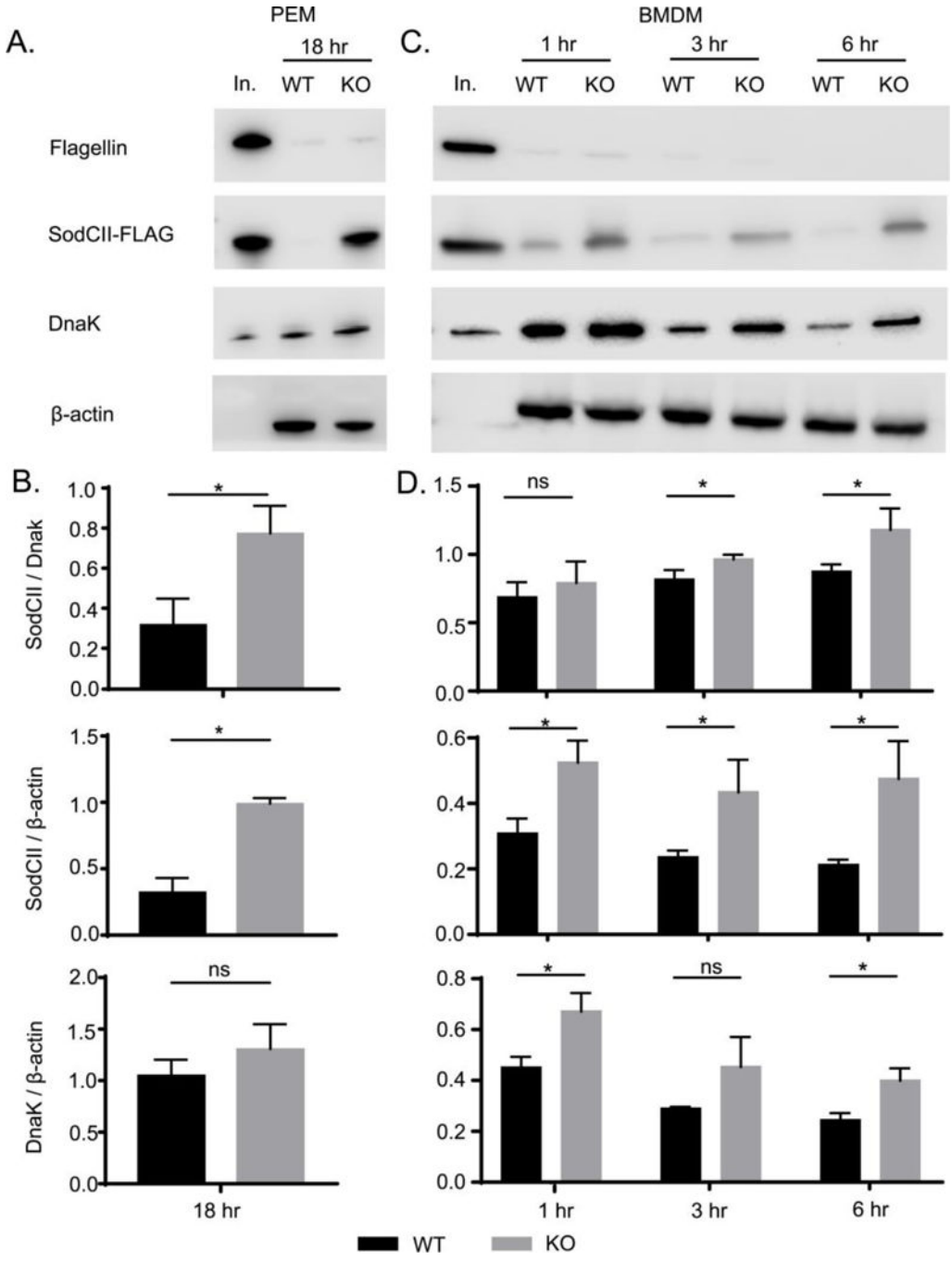

FIGURE 5.

Perforin-2 facilitates the degradation of antigens enclosed within the bacterial envelope**.** (A) PEMs isolated from Perforin-2 WT and KO mice were infected with a strain of *S.* Typhimurium expressing SodCII-FLAG. After 18 hours the phagocytosed bacteria were recovered and the indicated antigens were detected by Western blot. (B) Quantification of Western blot data from three separate experiments in PEMs. (C) Similar infection experiments were conducted with BMDM except the phagocytosed bacteria were recovered at 1, 3, and 6 hours post phagocytosis. (D) Quantification of Western blot data from three

separate experiments in BMDM. Means and standard deviations are shown; $n = 3$. Data were analyzed by two-way ANOVA with Sidack's multiple comparisons test. $*P \leq 0.05$.
Abbreviations: In., inoculum; ns, not significant

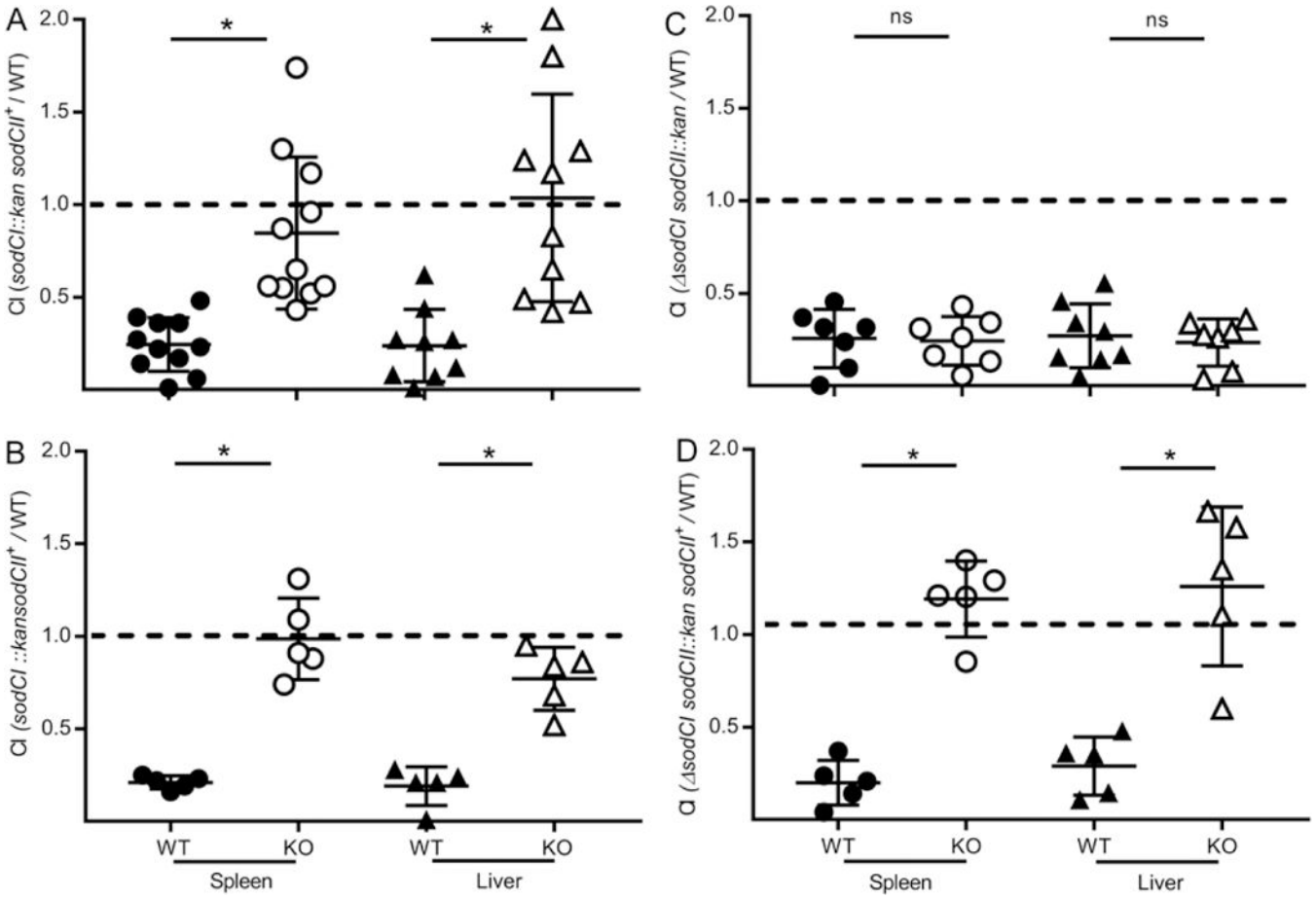

FIGURE 6.

SodCII is functional in Perforin-2 KO but not WT mice. WT and Perforin-2 KO mice were inoculated by intraperitoneal injection with *S.* Typhimurium WT strain GPM2004 and (A) Δ*sodCI::kan* strain ST188, (B) Δ*sodCI::kan* strain ST188b, (C) Δ*sodCI sodCII::kan* strain ST189 or (D) Δ*sodCI sodCII::kan sodCII*$^{+}$ strain GPM2008 at a 1:1 ratio. Organs were harvested 4 days post infection and strains enumerated on selective media. CI are derived from the ratios of mutant strains to WT strains with compensation for any differences in inocula. Medians and standard deviations are indicated by horizontal bars. $n = 5–11$. Data were analyzed by two-way ANOVA with Sidack's multiple comparisons test. $*P \leq 0.05$.

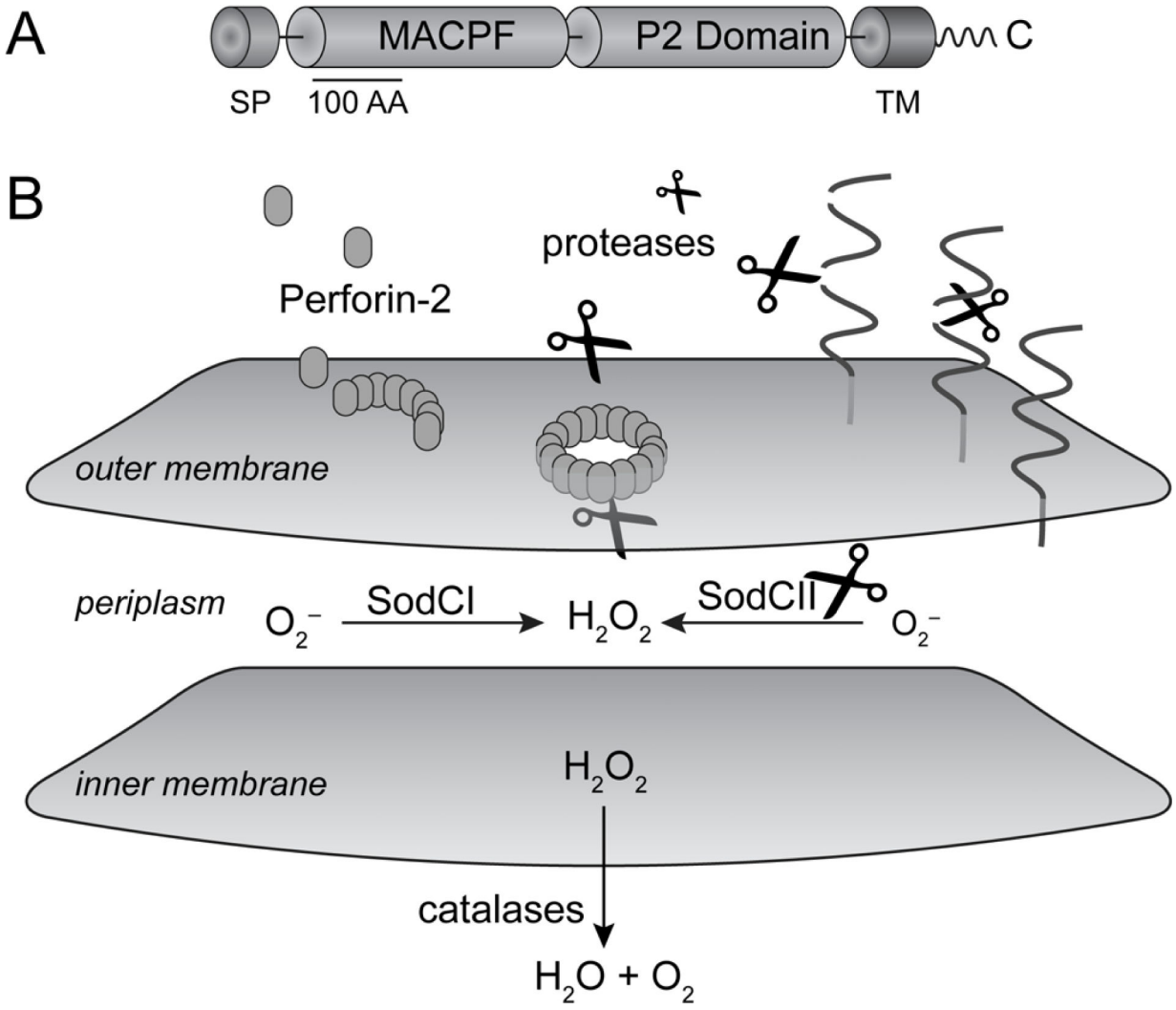

FIGURE 7.

Model for Perforin-2 dependent degradation of SodCII. (A) Domain organization of Perforin-2. MACPF domains are present in other proteins of the innate immune system and in the case of complement protein C9 and Perforin-1 have been shown to polymerize and form pores in lipid membranes. The P2 domain is a domain of unknown function that is conserved in orthologs of Perforin-2. As a type I transmembrane protein the MACPF domain of Perforin-2 would reside within the lumen of endosomes. (B) Upon activation and likely cleavage from its transmembrane domain Perforin-2 polymerizes on the outer membrane of *S.* Typhimurium. Subsequent pore formation allows proteases –and other antimicrobial effectors– to enter the periplasmic space and degrade SodCII. Alternatively, SodCII may diffuse through the poly-Perforin-2 pore and be destroyed in the lumen of the phagolysosome. Pores do not lead to the inactivation of SodCI because it is protease resistant and tethered within the periplasm. Abbreviations; SP, signal peptide; TM, transmembrane domain

Table 1

Bacteria strains

Strain	Description	Reference
LT2	Wild-type *S.* Typhimurium	(28)
LT2b	LT2 derivative that spontaneously lost pSLT virulence plasmid	this study
GPM2004	LT2 *attB*$_{\lambda}$::pCAH63, chloramphenicol resistant	this study
GPM2004b	LT2b *attB*$_{\lambda}$::pCAH63, chloramphenicol resistant	this study
ST188	LT2 Δ*sodCI::kan*	this study
ST188b	LT2b Δ*sodCI::kan*	this study
ST189	LT2 Δ*sodCI* Δ*sodCII::kan*	this study
GPM2008	LT2 Δ*sodCI* Δ*sodCII::kan attB*$_{\lambda}$::pAH63Tc-sodCII	this study
GPM2010	LT2 *attB*$_{\lambda}$::pCAH63, sfGFP and chloramphenicol resistant	this study
GPM2012	LT2 Δ*sodCI* Δ*sodCII::kan attB*$_{\lambda}$::pCAH63, sfGFP and chloramphenicol resistant	this study

Table 2

Oligonucleotide Primers

Primer	Sequence[a] (5'→3')
sodCI-P1	TACACAATATTGTCGCTGGTAGCTGGTGCGCTCATCAGTTGTGTAGGCTGGAGCTGCTTC
sodCI-P2	ATTGTCACCGCCTTTATGGATCATCAATGAGTGACCTTTCATATGAATATCCTCCTTAGT
sodCI-MfeI	TTTCAATTGATTAATGGTATTTACGATACAACC
sodCI-HindIII	TTTAAGCTTATGGCTATGTTGCTGTTATTTCTC
sodCII-P1	GCAGGCCGCCAGCGAGAAAGTAGAGATGAATCTGGTGACTGTGTAGGCTGGAGCTGCTTC
sodCII-P2	CGCCGCCGCCGAGCGGTTTCGGCTGATCGGACATGTTATCATATGAATATCCTCCTTAGT
sodCII-EcoRI	TTTGAATTCAACAGGCGACCACATGTAACGGAG
sodCII-HindIII	TTTAAGCTTCACTGGCTCCGGGTTATTTAATGA
1238	GCGTCTAGAGGGTTATGACGTGCCGTAATC
1239	GCGGGATCCTCTTCACTTGTCGTCATCGTCCTTGTAGTCTTTAATGACGCCGCAGGCGTAAC
1329	ACCCGGGGATCCTTTATGACGTGCCGTAATCGC
1330	TGTAGTCGAATTCTTTAATGACGCCGCAGGCGTAA
1331	CGGCGTCATTAAAGAATTCGACTACAAAGACCATGACG
1332	CAAAACAGCCAAGGGAACTTCGAAGCAGCTCCAG
1333	GCTTCGAAGTTCCCTTGGCTGTTTTGGCGGATGA
1334	CGGCACGTCATAAAGGATCCCCGGGTACCGAG
1584	CCAAGTCCAGCTATGGATAGCACTGAGAACGTC
1585	ATCGTAAGGGTACTGGAACAGGTGGTGGCG
1586	CACCTGTTCCAGTACCCTTACGATGTACCGG
1587	AGTGCTATCCATAGCTGGACTTGGATCCTCTTC
1426	CCTTACGATGTACCGGATTACGCATGAAGCTAGCTGGCCAGACATGATAAG
1427	GATTGCTTTGAATTAGCGGTGGTTTTCAC
1258	TGAATTAATGGCGATGACGCATC
1259	ATTATACGAGCCGGATGATTAATTGTCAACGCATGCAAGCTTGGCAC
1257	TCGTGAGGATGCGTCATCGCCATTAATTCAGCCAAGCTTCGAATTC
1243	GTTGACAATTAATCATCCGGCTCGTATAATCTACTGTTTCTCCATACCCG

[a]Underlined nucleotides indicate primer/template mismatches.